Baseband Carrier Recovery and Phase Tracking as a Doppler Compensation Technique for a zero-IF SDR

Ewald van der Westhuizen and Gert-Jan van Rooyen
Department of Electrical and Electronic Engineering, Stellenbosch University
Tel: 021-808-4481, Fax: 021-808-3951, Email: {ewald,gvrooyen}@dsp.sun.ac.za

***Abstract*—Compensating for the Doppler effect is a significant problem in low earth orbit (LEO) satellite communications. The effect of Doppler shift is that the baseband carrier signal is shifted in the frequency spectrum. This paper presents the design and analysis of a two-stage baseband carrier recovery algorithm for software-defined radio (SDR). The first-stage frequency-locked loop calculates a coarse estimate of the baseband carrier frequency. After a predetermined settling time, the coarse estimation stage switches to the second stage, in which fine tracking is performed by digital phase-locked loop. Two methods for the first-stage coarse carrier frequency estimation are compared. The first uses a feed-forward method, while the second method uses a feedback mechanism. The algorithms are implemented as part of an SDR modem running on a Freescale DSP56311 digital signal processor. Care is also taken in ensuring efficient implementation, e.g. by avoiding operations such as division, and by avoiding computationally intensive calculations.**

I. Introduction

Mobile communication systems, in particular low-earth orbit (LEO) satellite systems, are required to communicate reliably in the presence of Doppler frequency shift, which may move the received carrier substantially from its nominal frequency. In this paper, a carrier recovery system is considered that can reliably capture a received signal over a frequency range many times wider than the signal bandwidth. Furthermore, all compensation is performed in the digital domain in a software-defined radio (SDR). Consider the basic components of a digital communications system illustrated in Figure 1. The function of the SDR for data transmission is to convert digital data into a radio frequency (RF) signal suitable for transmission (modulation) and subsequently to extract digital data from a radio frequency signal (demodulation). All the SDR modulation, demodulation, Doppler compensation and mixing are performed in software running on a high-speed digital signal processor (DSP). The system described in this paper assumes that the RF front-end of the SDR is a quadrature mixer, implementing a zero-IF receiver [1].

We also assume a LEO satellite signal, in which significant Doppler shift is expected. For example, a LEO satellite communicating at 2.4GHz would achieve Doppler shift in the range of +96 kHz to –96 kHz when the satellite passes from horizon to zenith to horizon. The solution presented here assumes that the RF front-end of the SDR has already mixed the received signal spectrum down by the nominal carrier frequency shift, using quadrature downmixing. The resulting complex-valued time-domain signal would have a Fourier spectrum in which the desired signal is centred around the Doppler shift frequency. It is assumed that the rest of the downmixed spectrum (which was filtered prior to analogue-to-digital conversion) is comparatively quiet.[1] The proposed system first attempts to centre the bulk of the received signal energy at zero hertz, and then performs fine phase acquisition, in order to stabilise the received symbol constellation. Lastly, differential PSK is assumed, so that a constant error after phase lock has no effect on the demodulated data.

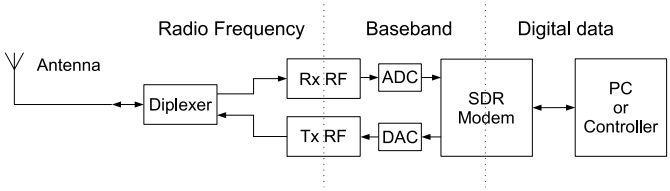

Fig. 1. Basic components in a communication system

A two-stage carrier recovery algorithm is implemented. The first stage (effectively a digital frequency estimator) is responsible for coarse carrier estimation while the second stage (a phase-locked loop) manages the fine-tuned phase tracking. Two alternative coarse carrier recovery (first stage) methods are considered, respectively using a feed-forward and a feedback approach. Finally Section IV presents performance results for the system over varying operational parameters.

II. Design

In order to maintain a narrow capture range for the second phase-locked loop stage (to improve lock stability), the received signal for the zero-intermediate frequency (zero-IF) receiver should be mixed down to a centre frequency of as close to zero hertz as possible. This is achieved through the first coarse carrier recovery phase.

Both coarse recovery methods presented here aim to estimate the carrier frequency of the modulated message signal. In theory the coarse carrier recovery techniques should be able to detect Doppler-shifted frequencies limited by the Nyquist criterion, i.e. $\frac{f_s}{2}$.

The application for which the software-defined baseband carrier recovery system was developed is a low-earth orbit, sun-synchronous satellite. Assuming an orbit height of $r_o =$

[1]This is reasonable if one assumes that the satellite communicates in a band that was licensed with the full Doppler shift in mind, or that potential disturbance signals are not Doppler-shifted, and may be filtered out in the analogue domain.

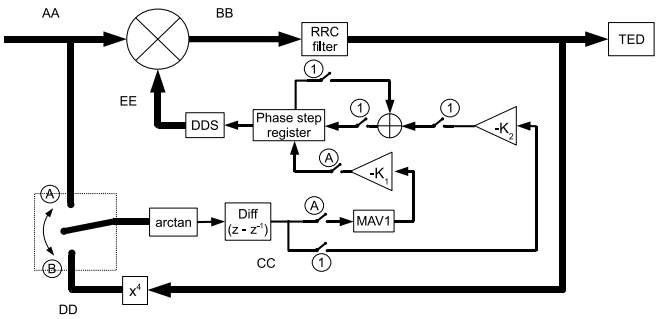

Fig. 2. Block diagram of feed-forward carrier recovery method

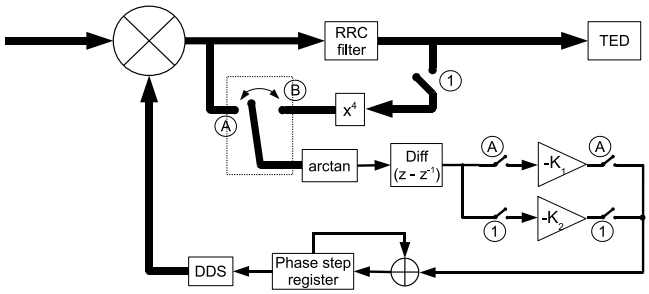

Fig. 3. Block diagram of feedback carrier recovery method

500 km and an average Earth radius of $r_e = 6\,371$ km, the satellite travels a distance of

$$s = 2\pi(r_e + r_o) = 43\,172 \text{ km}$$

per orbit. For sun-synchronous orbit, a full orbit is completed each hour, which implies a satellite speed of

$$v = \left(\frac{1000}{60 \cdot 60}\right) \cdot s = 11\,992 \text{ m/s}\,.$$

The maximum Doppler frequency shift is given as

$$\Delta f = \pm \frac{v}{c} f_0$$

which corresponds to ± 96 kHz for a carrier frequency of $f_0 = 2.4$ GHz. This worst-case Doppler frequency shift occurs only when the satellite is at the horizon, on an orbital trajectory that crosses zenith.

A. Coarse feed-forward carrier recovery

Figure 2 shows a block diagram of the feed-forward carrier recovery method. Thick arrow paths indicate complex-valued digital signals while thin arrow paths indicate a real-valued signal. The switch A/B switches between the two stages of operation. The signal path designated A indicates the coarse carrier recovery (first stage) operation. The second stage of operation is with the switch in position B. The switches numbered (1) are only in use during the second stage of operation and are left open when switch A/B is in position A. The working of stage two operation is discussed in a subsequent section.

The strategy behind this design is to estimate the average frequency of the sampled zero-IF input signal, which is presumed to have experienced a frequency shift away from zero hertz due to the Doppler effect. Consider signal path A. The input signal is the sampled baseband signal coming from the analogue-to-digital converters (ADCs) following the radio frequency receiver (Rx RF) section. The arctan of the complex-valued input signal is calculated in order to obtain the instantaneous phase of the signal. The instantaneous frequency of the signal can be determined from the rate of change of the phase. The discrete differential can be calculated to get an estimate of the frequency per sample. This is done by using Euler's method of approximating differential equations [3]. The estimate of the frequency is passed through a moving average filter (MAV1) to get a smoothed version of the differentiated signal, effectively extracting the average frequency of the input signal. The negative gain, $-K_1$, is used to convert the frequency signal to a negative phase accumulator step size for the direct digital synthesiser (DDS) [4]. The Doppler correction frequency is generated by the DDS at the negative of the estimated average input frequency. The input signal is mixed with the compensation signal in order to translate the baseband message signal spectrum closer to zero hertz. The downmixed analytic signal passes through the root raised cosine (RRC) filter. This filtered signal will subsequently be used by the second stage of operation for fine phase tracking.

B. Coarse feedback carrier recovery

Figure 3 shows a block diagram of the feedback carrier recovery method. Similar to the feed-forward method, the switch A/B controls the two-stage operation. The signal path with all the A-switches closed handles the coarse frequency recovery (first stage), while the fine phase tracking is done with the switch at position B. The switches numbered (1) are unused and left open when switch A/B is in position A.

Once again the input signal is the sampled baseband signal from the ADCs. It is mixed immediately with a compensation signal that is generated by the DDS. The aim of the mixing is to position the resulting signal at zero hertz. The frequency of the signal after mixing will be at an offset error frequency if the frequencies of the input and compensation signals do not sum to zero. This error frequency is estimated, fed back negatively, and used to update the compensation signal frequency.

Consider the signal path A that the signal at the offset error frequency follows. The angle of the complex-valued signal sample is calculated to get the instantaneous phase of the error signal. The error frequency per sample is calculated by taking the discrete differential of the instantaneous phase. A negative gain, $-K_1$, is applied to the calculated error frequency. The gain controls the response time and stability of the feedback loop and negatively feeds back the error frequency control signal to the DDS. The updating of the phase step register is arranged as a discrete integrator (accumulator) and continually tries to adjust and maintain the error frequency at zero hertz. After the error frequency settles at around zero hertz, fine phase tracking is activated.

C. Effect of the message signal on coarse carrier estimation

The message signal has an undesirable effect on accurate baseband carrier frequency estimation. The pulse-smoothed

phase modulated message signal has a continually changing frequency response over a relatively short time frame in the order of the symbol rate. These perturbations cause undesirable spikes in the frequency estimate. The moving average filter is used to lessen the effect of the undesirable spikes.

D. Fine feedback phase tracking

In both Figures 2 and 3 the signal paths with switch A/B in position B are identical. The switches numbered (1) are only closed at symbol sampling times and has the effect of downsampling the message signal to the symbol rate.

Assume the signal after mixing is

$$s(t) = e^{j[\omega_d t + \phi(t)]}$$

where ω_d is the undesired frequency offset (presumably due to Doppler shift) and $\phi(t)$ is the modulation information. In the case of QPSK, the phase modulation term, $\phi(t)$, represents a pulse-shaped signal that varies in phase at the symbol rate. At the exact symbol centres, ϕ can be represented as

$$\phi(n) = nk\frac{\pi}{2},\ n \in \mathbb{Z},\ k = [0; 1; 2; 3]$$

where n is the symbol number and k the symbol value which is either 0, 1, 2 or 3. Raising $s(t)$ to the fourth power results in it having a four times higher offset frequency and the phase modulation term becoming

$$4\phi(n) = nk2\pi,\ n \in \mathbb{Z},\ k = [0; 1; 2; 3]$$

at QPSK symbol positions. The signal is then downsampled, synchronised at the symbol centres. At the symbol positions the frequency offset can be best observed as this is where the phase modulation term, $4\phi(n)$, falls away and has no effect. The phase of the signal, $4\omega_0 t$, is obtained by applying the arctan function. The phase is differentiated to obtain the offset frequency value, $4\omega_0$. A gain, $-K_2$, is applied which converts the frequency value to a compensation phase accumulator step. The accumulator (digital integrator) enables tracking of linear phase changes and aims to keep the frequency offset value at zero. The DDS generates the compensation signal. The loop is closed where the frequency offset signal is mixed with the compensation signal in order to place the message signal at DC.

A Gardner [6] timing-error detector (TED) is used to synchronise the message signal with the intended symbol sample positions. The advantage of using this TED is that it uses very little memory as it only needs three sample values per symbol to calculate an estimate of the symbol position error. The TED is used to control the closing of the switches labelled (1) in Figures 2 and 3 enabling the PLL to only consider the phase at the intended symbol positions.

E. A/B-switch decision rule

Switching between the first and second stages of operation is kept simple. A transition from A to B (coarse to fine operation) is determined heuristically, and switches after the suitable settling time of either the moving average filter (feed-forward) or the settling time of the feedback loop is reached.

TABLE I
SYSTEM DESIGN PARAMETERS

Parameter	**Value**
Modulation scheme	Differential QPSK
Sampling rate (f_s)	230.4 kS/s
Symbol rate (R_{sym})	19 200 sym/s
Samples per symbol	12
Bits per symbol	2
Baseband carrier frequency (f_c)	19 200 Hz
Worst-case Doppler shift	$\pm$96 kHz
Duration of LEO satellite communication window	5 minutes
Rate of frequency change (phase acceleration) during satellite pass	$\sim$ 640 Hz/s

A transition from B to A (fine to coarse) occurs either when lock of the fine phase tracking is lost or when suitable lock is not obtained after a transition from coarse to fine tracking. During fine tracking, the energy of the frequency control signal over a finite time frame is monitored and compared to a threshold, thereby determining whether suitable lock is obtained and maintained. The value of the threshold was determined experimentally. Whenever the energy threshold is crossed, fine tracking switches back to coarse carrier recovery.

F. Fine phase tracking capture range

The sample rate during fine phase tracking is equal to the symbol rate, R_{sym}. Frequencies lower than $\frac{R_{\mathrm{sym}}}{2}$ can be fully represented without aliasing (Nyquist criterion). The power of four operation used in fine phase tracking further narrows the capture range of the phase-locked loop. The frequency multiplication by four makes aliasing become apparent already at frequencies four times lower than the frequency before the power of four operation. This brings the capture range down to $\frac{R_{\mathrm{sym}}}{8}$.

III. IMPLEMENTATION

The SDR is implemented on a Freescale DSP56311 in the C programming language. Care is taken to avoid computationally demanding operations such as division and floating point calculations. Settling times controlling the A/B-switch decision rule were chosen experimentally as follows from the discussion of the results in Section IV. The same applies for suitable choices for feedback gain values for both the coarse feedback and fine phase tracking methods. Table I lists the design parameters for the system.

A. Implementation of a FIR moving average filter

A simple moving average filter is given by the equation [7]

$$y(n) = \frac{1}{N}\sum_{k=0}^{N-1} x(n-k)$$

where N is the filter length and x represents input sample values in a buffer containing the current input value, $x(0)$, and $N-1$ past input values. Division by N is done to obtain the average value, $y(n)$. Since the moving average

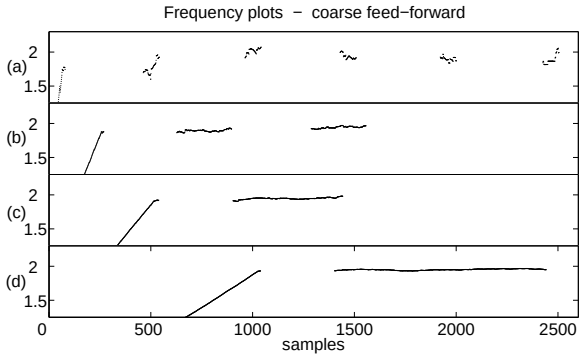

Fig. 4. Frequency plots during coarse frequency estimation for various moving average filter lengths (a) $N = 64$ (b) $N = 256$ (c) $N = 512$ (d) $N = 1024$.

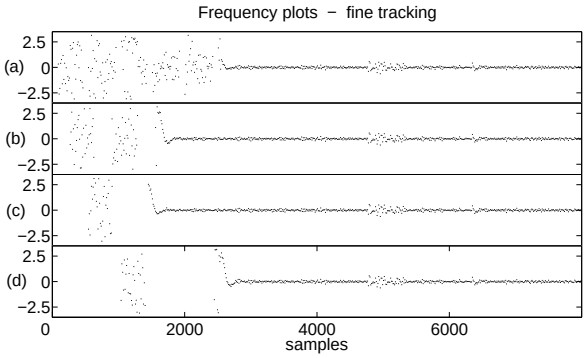

Fig. 5. Frequency plots during fine phase tracking for various moving average filter lengths (a) $N = 64$ (b) $N = 256$ (c) $N = 512$ (d) $N = 1024$.

operation is used in more that one instance in the SDR, an efficient implementation is preferred. For this reason the filter is implemented without the division operation and only the sum is considered. Another optimisation is that the summation over all the input buffer elements is not performed at every call of the moving average function. Instead, a static variable containing the sum is updated during each function call. The update to the sum variable subtracts the oldest input value in the input buffer and adds the current input value.

An adjustment is made to the gain values following the moving average operation to compensate for the fact that the division operation is omitted.

IV. Results

A. Coarse feed-forward carrier recovery

Figure 4 shows plots of simulation results of frequency tracking signals during coarse frequency estimation while attempting to switch from coarse to fine tracking. In each figure, the four plots (a) to (d) show the results for the four moving average filter lengths considered. It is clear from the frequency plots that the longer the filter length the smoother the resulting frequency estimate and the lower the effect of the perturbations caused by the message signal.

The white space intervals between the more continuous sections in Figure 4 are the sections where fine tracking attempts to lock on the phase. In Figure 4(a) five unsuccessful fine tracking lock attempts are observed. Only at the sixth attempt lock is obtained. The reason why lock is not obtained during the first five attempts is because coarse frequency estimation for $N = 64$ does not provide sufficient smoothing and after switching to fine tracking the estimated frequency falls out of the capture range to successfully obtain lock. The deviations in frequency caused by the message signal are significant. The frequency estimate becomes more accurate with larger values of N and fine tracking lock is obtained after fewer attempts at the cost of a longer settling time for the moving average filter.

Figure 5 shows the accompanying fine phase tracking frequency signal plots. The dispersed dots at the onset of each plot show that lock is not obtained. As the input signal moves into capture range, a steep adjustment and small overshoot may be observed, after which the frequency signal settles around zero.

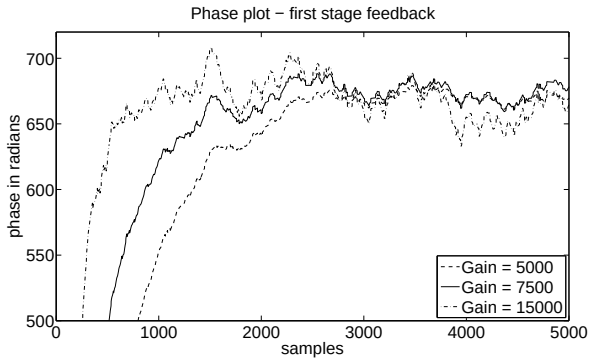

Fig. 6. Coarse feedback phase with gains

Results with regards to fine tracking gain and overshoot are discussed in Section IV-D.

B. Coarse feedback carrier recovery

Figure 6 shows the the phase signal for different coarse feedback carrier recovery gains. It can be observed that the phase signal is less erratic for lower gains after the phase signal has settled. This is preferable but comes at the cost of a longer settling time. The lower gain is not so susceptible to the disturbances caused by the message signal. The frequency signal plot in Figure 7 clearly shows how the frequency settles around zero hertz and how the message signal causes spike-like disturbances in the signal. The fact that the message signal at least causes regular zero crossings in the frequency signal helps the fine tracking method to obtain lock after the switch from coarse to fine tracking.

The graph in Figure 8 shows the settling time with respect to the feedback gain. The settling time, given in samples, is calculated as the time taken for the signal to settle to 5% of the initial value. As the gain increases the settling time decreases as expected.

C. Coarse feed-forward versus coarse feedback

Both coarse frequency estimation methods bring the message signal within capture range for successful fine phase locking. What distinguishes the one method from the other lies in the ability to adjust the available parameters of the respective

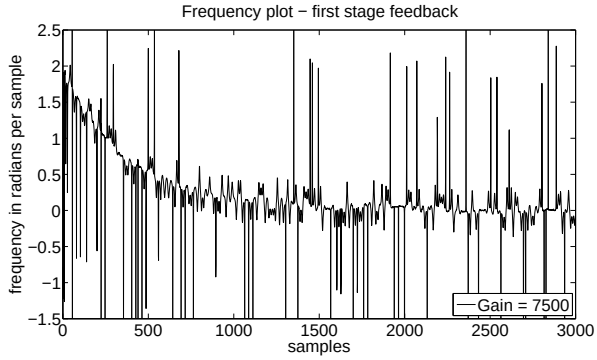

Fig. 7. Coarse feedback frequency with gains

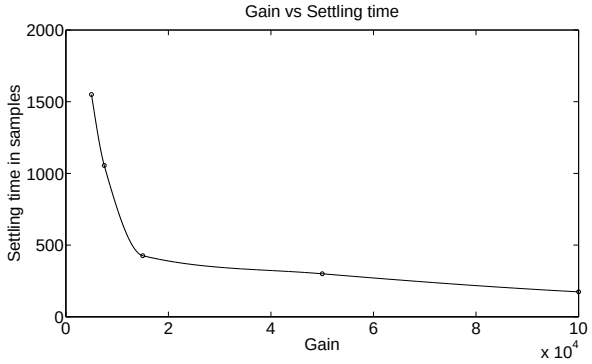

Fig. 8. Plot of coarse feedback gain against measured settling time.

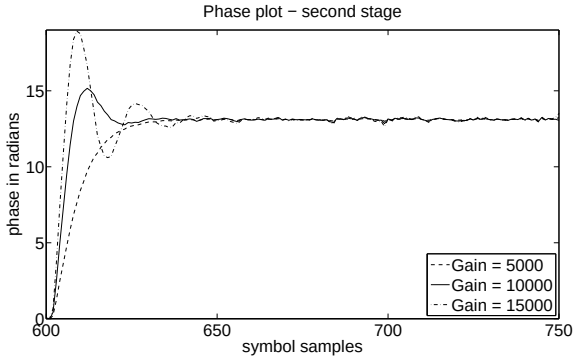

Fig. 9. Fine phase tracking phase signal response for varying gains.

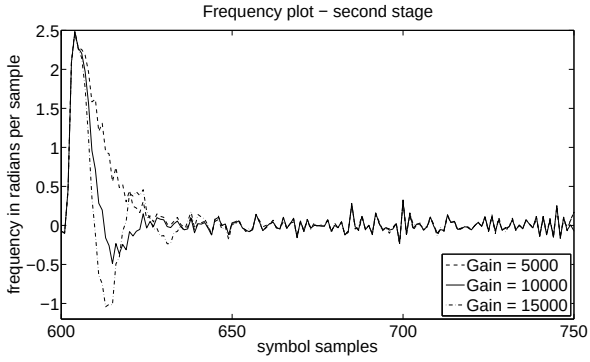

Fig. 10. Fine phase tracking frequency signal response for varying gains.

method to the needs of the application. Parameters that can be adjusted in the the feed-forward technique include the moving average filter length and settling time. The moving average filter length determines the smoothness of the frequency signal, and thus how severe the the effect of message signal disturbances is affecting the cature range of the PLL. The settling time for the moving average filter can be optimised independent of the moving average filter length which is an advantage if it is required that the frequency estimate time should be extremely short. The coarse feedback technique is limited in that only the feedback gain can be adjusted, affecting both the settling time and capture range of the frequency signal.

D. Fine feedback phase tracking

The effect of different fine tracking feedback gain values on phase and frequency settling times are shown in Figures 9 and 10. Overshoot in the phase settling can be seen for high gains while lower gains tend to have no overshoot with longer settling times. A gain of 10 000 gave reasonable overshoot while settling within roughly 25 symbols.

V. Conclusion

A two-stage carrier recovery algorithm was implemented, and two course frequency recovery methods were investigated. It was demonstrated that Doppler compensation can be performed in the digital domain with reasonably low computational complexity, removing the need for complex analogue compensation techniques. The technique that was implemented performs blind estimation of the Doppler shift, and does not require any information on the position, trajectory or velocity of the remote transmitter.

The purpose of the simulations presented here was to test the viability of the concept in ideal conditions. Further work includes tests in noisy conditions and in the presence of interfering transmissions, as well as the practical implementation and verification of the technique.

References

[1] W. Tuttlebee, *Software Defined Radio*, West Sussex: Wiley, 2002.

[2] R.E. Ziemer and W.H. Tranter, *Principles of Communications: Systems, Modulation and Noise*, Fourth edition. New York: John Wiley & Sons, 1995.

[3] Gene F. Franklin, J. David Powell and Michael Workman, *Digital Control of Dynamic Systems*, Third Edition. Menlo Park, CA: Addison Wesley Longman, Inc., 1998.

[4] J. Vankka, "Methods of Mapping from Phase to Sine Amplitude in Direct Digital Synthesis," *IEEE Transactions on Ultrasonics, Ferroelectrics, and Frequency Control*, vol. 44, no. 2, pp. 526–534, March 1997.

[5] B. Razavi, "Design Considerations for Direct-Conversion Receivers," *IEEE Transactions on Circuits and Systems II: Analog and Digital Signal Processing*, vol. 44, no. 6, pp. 428–435, June 1997.

[6] F.M. Gardner, "A BPSK/QPSK Timing-Error Detector for Sampled Receivers," *IEEE Transactions on Communications*, vol. COM-34, pp. 423–429, May 1986.

[7] John G. Proakis and Dimitris G. Manolakis, *Digital Signal Processing: Principles, Algorithms, and Applications*, Third Edition. London: Prentice-Hall International, 1996.

[8] Steven P. Nicoloso, *An Investigation of Carrier Recovery Techniques for PSK Modulated Signals in CDMA and Multipath Mobile Environment*, Master Thesis, Virginia Polytechnic Institute and State University

[9] ITU, *Handbook on Satellite Communications*, Third Edition, John Wiley & Sons, Incorporated, 2002

Ewald van der Westhuizen grew up in the Southern Cape. He completed both his B.Eng (2000) and M.Sc.Eng (2003) degrees in Electronic Engineering at Stellenbosch University. He worked for a Boston, MA based company in the fields of audio and video compression and rich media applications for mobile phones while residing in Cape Town. He is currently employed at Stellenbosch University as a Project Engineer.

Gert-Jan van Rooyen received his BEng in Electronic Engineering from Stellenbosch University in 1998, and completed his PhD at the same institution in 2005. He is currently Senior Lecturer in Telecommunications and Signal Processing at Stellenbosch University, and his current research activities include communication systems, radar and electronic media technology.